ORIGINAL ARTICLE

# Semi-synthetic chondroitin sulfate CS-semi5 upregulates miR-122-5p, conferring a therapeutic effect on osteoarthritis *via* the p38/MMP13 pathway

Xiang Li [a,†], Ya Zhou [a,†], Xuefeng Chen [a], Hongjun Wang [b], Shuang Yang [a], Jun Yang [b], Yunfeng Song [c], Zhehui Zhao [a,*], Haijing Zhang [a,*], Lianqiu Wu [a,*]

[a]*State Key Laboratory of Digestive Health, Institute of Materia Medica, Chinese Academy of Medical Sciences and Peking Union Medical College, Beijing 100050, China*
[b]*Tide Pharmaceutical Co., Ltd., Beijing 100176, China*
[c]*Camford Royal School, Beijing 100093, China*

**Abstract** Osteoarthritis (OA) is an aging-associated disease characterized by joint stiffness pain and destroyed articular cartilage. Traditional treatments for OA are limited to alleviating various OA symptoms. There is a lack of drugs available in clinical practice that can truly repair cartilage damage. Here, we developed the chondroitin sulfate analog CS-semi5, semi-synthesized from chondroitin sulfate A. *In vivo*, CS-semi5 alleviated inflammation, provided analgesic effects, and protected cartilage in the modified Hulth OA rat model and papain-induced OA rat model. A bioinformatics analysis was performed on samples from OA patients and an exosome analysis on papain-induced OA rats, revealing miR-122-5p as the key regulator associated with CS-semi5 in OA treatment. Binding prediction revealed that miR-122-5p acted on the 3′-untranslated region of p38 mitogen-activated protein kinase, which was related to MMP13 regulation. Subsequent *in vitro* experiments revealed that CS-semi5 effectively reduced cartilage degeneration and maintained matrix homeostasis by inhibiting matrix breakdown through the miR-122-5p/p38/MMP13 axis, which was further validated in the articular cartilage of OA rats. This

---

*Corresponding authors.
    E-mail addresses: wlq@imm.ac.cn (Lianqiu Wu), zhaozh@imm.ac.cn (Zhehui Zhao), zhanghaijing@imm.ac.cn (Haijing Zhang).
†These authors made equal contributions to this work.

is the first study to investigate the semi-synthesized chondroitin sulfate CS-semi5, revealing its cartilage-protecting, anti-inflammatory, and analgesic properties that show promising therapeutic effects in OA *via* the miR-122-5p/p38/MMP13 pathway.

## 1. Introduction

Osteoarthritis (OA) is a slow, progressive disease characterized by a morphology and function change of whole joint parts such as articular cartilage, synovium, and subchondral bone. The incidence of OA is increasing annually as the global population aging and the prevalence of associated factors, including diabetes, weight, and so on. It is estimated that 240 million individuals worldwide have symptomatic OA, including 10% of men and 18% of women over age 60. The prevalence of symptomatic knee OA was 7% among adults aged $\geq$45 years in the US[1]. A recent meta-analysis revealed that symptomatic knee OA prevalence in China was approximately 14.6%[1,2].

Traditional treatments for OA, such as nonsteroidal anti-inflammatory drugs (NSAIDs), intra-articular corticosteroids, acetaminophen/paracetamol, and opioid analgesics are mainly used to alleviate various OA symptoms rather than prevent disease progression[3]. Therefore, effective drugs for OA are sharply lacking, especially those that protect the cartilage and address the etiology of the disease rather than simply alleviating symptoms. Symptomatic slow-acting drugs for OA including chondroitin sulfate and glucosamine sulfate are widely used from country to country[4]. Oral glucosamine sulfate, chondroitin sulfate (CS), and injectable sodium hyaluronate are cartilage protectants that can alleviate OA symptoms, improve function, and delay structural progression with long-term use[5-7]. However, the clinical efficacy of cartilage protectants remains controversial, and studies across different countries have produced contradictory results[8,9]. Various concernings are arising for long-term use adverse reactions and inconsistent natural resources in researches[10,11]. Different clinical trials have revealed that the therapeutic effects of chondroitin sulfate may depend on many variables, such as the source of origin, purity, and contamination with by-products[3,4]. CS is often combined with glucosamine, which makes it difficult to confirm the specific contribution of CS to the therapeutic effect on OA[5]. CS researchers are currently investigating the biological effects and efficacy of CS and the proper standardization of CS quality for clinical efficacy in OA[9].

CS is the basic component of cartilage and synovial fluid. CS comprises 40−200 repeating disaccharide units and is a sulfated linear polysaccharide of the glycosaminoglycan (GAG) family[5]. Numerous studies have shown that most chondroitin sulfate proteoglycan (CSPG) functions arise from CS molecules. CS stimulates cartilage metabolism by increasing the synthesis of collagen II (COL II) and proteoglycan and acts on cartilage, synovium, and subchondral bone to repair damaged joint structures. CS also plays an anti-inflammatory role by inhibiting the secretion of pro-inflammatory factors and proteases and improving the synthesis and metabolic balance of the extracellular cartilage matrix[6,7]. CS also can delay cartilage degradation caused by inflammation and reduce the levels of matrix metalloproteinases (MMPs), including MMP-3, MMP-9, and MMP-13. CS acts on CD44 and intercellular cell adhesion molecule-1 to dephosphorylate p38 mitogen-activated protein kinase (MAPK) and extracellular signal-regulated kinase 1/2, thereby reducing nuclear factor kappa-B nuclear translocation, subsequently inhibiting OA progression. In addition, CS increases transforming growth factor-$\beta$ expression, promoting the synthesis of high molecular weight hyaluronan and COL II[3].

CS has many subtypes with varying sulfation patterns, resulting in high heterogeneity and complexity (Fig. 1A). CS is also mainly extracted and purified from the cartilage of different animals before application; thus, the purity varies, affecting the biological effects and clinical efficacy. Commercial CS GAG is generally derived from bovine and porcine (CS-A), and shark (CS-C) cartilage. Moreover, rare forms of CS have been obtained from other species, such as crab, squid, and hagfish. CS-E with the best biological activity, obtained from squid cartilage, contains substantial quantities of other forms of CS, complicating the extraction and purification process and substantially increasing its cost.

In this study, using CS-A as the raw material, we synthesized a series of CS polysaccharides with different degrees of sulfation and studied the relationship between biological activity and the sulfation degree and position. We identified the semi-synthesized sulfated CS CS-semi5 as a promising OA therapeutic and evaluated its biological and therapeutic mechanisms, revealing potential clinical efficacy.

## 2. Materials and methods

### 2.1. Materials

CS-A from bovine trachea was purchased from Yantai Dongcheng Pharmaceutical Group Co., Ltd. (Yantai, China). Trimethylamine sulfur trioxide was purchased from 3A (Shanghai, China). Croton oil was purchased from Tokyo Chemical Industry Co., Ltd. (Tokyo, Japan). Ethanol (95%), ether, glacial acetic acid, and 0.9% sodium chloride were purchased from Sinopharm Chemical Reagent Beijing Co., Ltd. (Beijing, China). Dexamethasone acetate was purchased from Selleck Chemicals (Houston, USA). Diclofenac was purchased from Novartis Pharma (Switzerland). Cell counting kit-8 (CCK8) and 4% paraformaldehyde were purchased from Lablead Biotech Co., Ltd. (Beijing, China). Dulbecco's modified Eagle's medium, phosphate-buffered saline (PBS), guanidine hydrochloride, and Alcian blue stain kit were purchased from Solarbio Science and Technology, Co., Ltd. (Beijing, China). P38 MAPK inhibitor SB203580 was purchased from MedChemExpress (Monmouth Junction, NJ, USA). Fetal bovine serum, penicillin, and streptomycin were purchased from
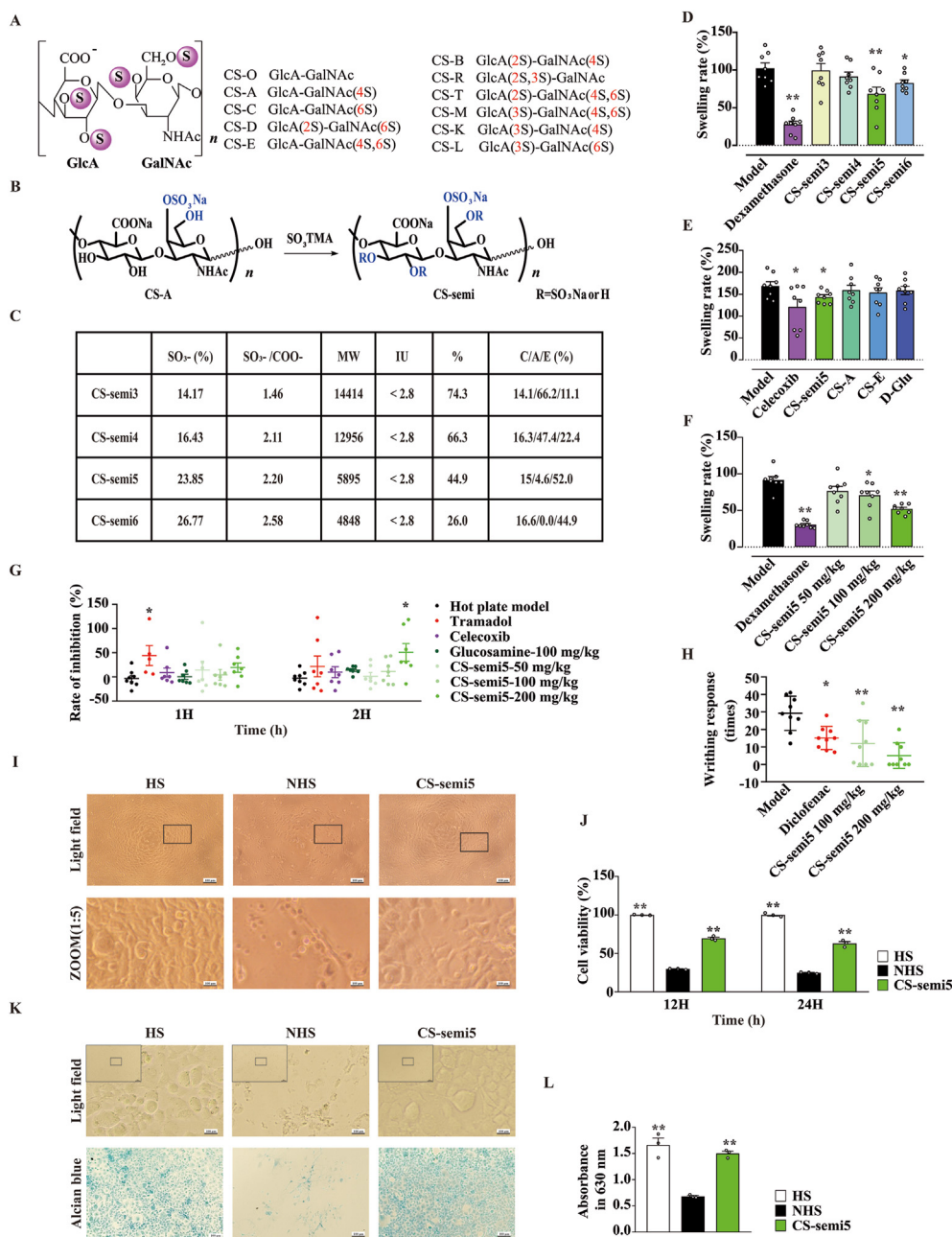
**Figure 1** The structure−activity relationship and preliminary activity of CS-semi5. (A) Different types of CS. (B) Synthesis of CS-semi compounds. (C) The characteristics of various CS-semi compounds. (D) CS-semi5 had the best anti-inflammatory activity among the CS-semi series compounds ($n = 8$). (E) CS-semi5 had a better anti-inflammatory effect than CS-A and D-Glu ($n = 8$). (F) CS-semi5 inhibited inflammation in a dose-dependent manner ($n = 8$). (G) CS-semi5 exhibited analgesic activity in the hot plate test ($n = 8$). (H) CS-semi5 effectively inhibited acetic acid-induced pain ($n = 10$); *$P < 0.05$ and **$P < 0.01$ compared with the Model group. (I) CS-semi5 protected primary chondrocytes from complement-induced death (scale bar: 100 μm). The black box represents the enlarged part of the original image. (J) Quantitative results of the complement-induced death experiment ($n = 3$); *$P < 0.05$ and **$P < 0.01$ compared with NHS group. (K) CS-semi5 improved primary chondrocytes extracellular matrix from complement-induced death (scale bar: 100 μm). The black box represents the enlarged part of the original image. (L) Quantitative results of the Alcian blue staining of extracellular sulfated GAGs ($n = 3$); *$P < 0.05$ and **$P < 0.01$ compared with NHS group.

Gibco Life Technologies (Carlsbad, CA, United States). Papain and L-cysteine were purchased from Sigma−Aldrich Co. (St. Louis, MO, USA). Enzyme-linked immunosorbent assay (ELISA) kits were purchased from R&D Systems, Inc. (Minneapolis, MN, USA). Recombinant mouse interleukin-1β (IL-1β) was purchased from Peprotech (Rocky Hill, NJ, USA).

### 2.2. Semi-synthesis of CS-semi

A mixture of CS-A (26.8 g, 0.05 mol) in 200 mL of dimethyl sulfoxide (previously dried over 4 Å molecular sieves) was added to trimethylamine sulfur trioxide (2−6, 8 equiv. free hydroxyl group, based on disaccharide units). The mixture was stirred vigorously at

60 °C for 24 h to achieve a clear solution. The reaction solution was allowed to cool to room temperature, which was then transferred into a solution of sodium acetate in ethanol (2%, 1000 mL) at room temperature. The precipitate was formed, filtered off, and washed with 100 mL ethanol to produce CS-semi as a brown solid. The crude polysaccharides were dissolved into 200 mL water, with 4 mol/L NaOH to adjust the pH to neutral. The solution was then dialyzed against distilled water for 2 days, and the dialysate was lyophilized to produce CS-semi as an off-white solid.

### 2.3. Ethics approval statement

The animal experimental procedures were conducted strictly following the Guide for the Care and Use of Laboratory Animals (National Institutes of Health publication 85-23, revised 1985) and approved by the Experimental Animal Welfare and Ethics Committee of the Institute of Materia Medica, Chinese Academy of Medical Sciences.

### 2.4. Animals

Kunming mice (male, 20−22 g), Institute for Cancer Research (ICR) mice (female, 18−20 g), Sprague−Dawley (SD) rats (male, 180−200 g), and neonatal C57BL/6 mice (4−7 days) were purchased from Vital River Laboratories. All animals were raised in individually ventilated cages with standard food and water provided *ad libitum* under controlled specific pathogen-free (SPF) conditions (25 °C, 55% humidity, 12-h light/dark cycle). All animals were acclimatized for one week before experimentation.

### 2.5. Croton oil-induced ear edema test

Anti-inflammatory activity was measured using an ear edema experiment. The ear edema experiment was performed on animals treated orally with distilled water (100 mg/kg, negative control group), dexamethasone acetate (0.25 mg/kg, positive group), or a series of different compounds ($n = 8$). Male Kunming mice in each group were administered the respective compounds twice before ear edema was induced in the right ear with 20 μL 2% Croton ether solution. The left ear remained untreated. After 4 h, the animals were killed by cervical dislocation, and a 6 mm diameter representative disc was taken from each ear. The weight differences between the control ear discs (left) and the Croton oil-treated ear discs (right) were determined using an analytical balance. The ear edema rate was calculated with Eq. (1):

Ear edema rate (%)= (Right disc weight−Left disc weight)/(Left disc weight) × 100     (1)

### 2.6. Hot plate test

A hot plate test was used to assess antinociceptive activity. The temperature of the metal surface was set at $50 \pm 0.1$ °C. Latency was measured when the animal licked its back paw or jumped off the plate to avoid thermal pain. Screened female ICR mice with a latency of 5−30 s were randomly divided into 4 groups: the control, tramadol (15 mg/kg), CS-semi5 (100 mg/kg), and CS-semi5 (200 mg/kg) groups ($n = 8$). The latencies were measured at 0, 1 and 2 h after administration.

### 2.7. Acetic acid-induced abdominal writhing test

An acetic acid-induced writhing test was conducted to evaluate the analgesic effect of the tested drugs. Male ICR mice were divided into four groups ($n = 10$): the negative control (normal saline, 10 mL/kg), positive control (diclofenac, 10 mg/kg), CS-semi5 (100 mg/kg), and CS-semi5 (200 mg/kg) groups. Mice pre-received diclofenac (10 mg/kg) or CS-semi5 (100 and 200 mg/kg) orally before the acetic-acid writhing test. After 1 h of administration, 1.0% acetic acid solution (10 mL/kg) was injected into each mouse intraperitoneally. The writhing incidence was quantified over 15 min by investigators blinded to the drug treatment groups. Analgesic activity was assessed as the analgesic rate calculated using Eq. (2):

Analgesic rate (%) = [(Writhing times (negative control group)−
    Writhing times (drug experimental group)]/Writhing times
    (negative control group) × 100     (2)

### 2.8. Primary chondrocyte culture

Primary chondrocytes were isolated from 4 to 7 day-old neonatal mice. After being sacrificed, the mice were disinfected with 75% alcohol. Then, the skin and muscle were cut with scissors to expose the joint capsule, and the white translucent articular cartilage of the femur and tibia was removed. The cartilage tissue was cut into fragments and digested with 0.25% trypsin for 30 min. The samples were subsequently incubated in 0.2% collagenase II for 2 h. Filtered chondrocytes were cultured in Dulbecco's modified Eagle's medium/F12 medium with 20% fetal bovine serum in a humidified atmosphere and 5% $CO_2$ at 37 °C.

### 2.9. Complement test

Primary mouse chondrocytes were treated with or without CS-semi5 (1 mg/mL) and 40 μL non-heated human serum (NHS) donated by our investigators in 96-well plates; a control group was treated with 40 μL heated human serum (HS). Then, the plates were incubated at 37 °C and 5% $CO_2$ for 24 h, and the cell viability was measured by cell counting kit-8 (CCK-8) and Alcian blue staining.

### 2.10. CCK-8 assay

CCK-8 was used to measure the cytotoxicity of CS-semi5 in primary chondrocytes and the viability of chondrocytes in the complement test. Cells were seeded in 96-well plates for 24 h, CCK-8 reagent was added, and the plates were then incubated for another 3 h. The absorbance was measured at 450 nm with a microplate reader (BioTek, Winooski, USA).

### 2.11. Alcian blue staining

Alcian Blue is a dye used to detect cell chondrogenesis and it stains the sulfated proteoglycan in cartilage tissue. It can clearly display the morphology and structure of chondrocytes, especially the state of the extracellular matrix. After complement-induced death for 24 h, the plate was taken out and used to perform the Alcian blue staining. The plate was washed with PBS twice, fixed

with 4% paraformaldehyde for 30 min, acidified with sulfuric acid, and stained with Alcian blue solution according to manufacture protocols. The results of Alcian blue staining were photographed and then 6 mol/L guanidine hydrochloride solution was added to extract the staining materials and the supernatant was obtained to detect the absorbance in 630 nm.

### 2.12. Detection of MMP13

Primary mouse chondrocytes were seeded into 96-well culture plates at 5000 cells/well. After overnight culture, the cells were incubated with IL-1$\beta$ (10 ng/mL) and CS-semi5 (0.1, 1 and 10 mg/mL) for 24 h. The supernatant was subsequently collected for MMP-13 detection by ELISA following the manufacturer's protocol.

### 2.13. Western blotting

Primary mouse chondrocytes were seeded into 6-well culture plates at 100,000 cells/well, incubated for 24 h, and treated with IL-1$\beta$ (10 ng/mL) and CS-semi5 (0.1, 1, 10 mg/mL) for another 24 h. Total protein was obtained from cell lysates in a loading buffer, and the concentration was measured using a BCA protein assay. Equal amounts of protein were separated by sodium dodecyl sulfate polyacrylamide gel electrophoresis and transferred to nitrocellulose membranes. After 1 h of blocking, the membranes containing the protein were cut and incubated with the indicated primary antibody overnight at 4 °C. On the second day, the samples were incubated in secondary antibodies for 1 h at room temperature. The membranes were then incubated with enhanced chemiluminescence solution to visualization of the proteins.

### 2.14. Immunofluorescence analysis

Primary mouse chondrocytes cultured on confocal culture dishes at 5000 cells/dish were washed with PBS. Then, they were fixed with 4% paraformaldehyde for 30 min and permeabilized using 0.1% Triton X-100 for 15 min. The cells were blocked for 1 h in 10% goat serum and thereafter incubated overnight in appropriately diluted primary antibodies. The next day, after three washes with PBS, fluorescein-labeled goat anti-rabbit IgG antibody was added, and the samples were incubated in the dark at room temperature for 1 h. Subsequently, the cells were rinsed with PBS three times and stained with 4′,6-diamidino-2-phenylindole (DAPI). Images were taken using a laser scanning confocal microscope (Leica TCS SP8X).

### 2.15. Modified Hulth model in rats

The anti-OA effect of CS-semi5 was preliminarily evaluated in modified Hulth model rats established as follows. Briefly, the SD rats were anesthetized and the skin at the knee joint was incised. The joint was cut from the medial edge of the patella, and the patella with the ligament attached was removed, exposing the capsule. The anterior cruciate ligament and the medial meniscus were subsequently excised, and the meniscus of the knee joint was removed. After modeling, the articular cavity was rinsed, the patella was reset, and the joint cavity and skin incisions were sutured.

Penicillin (200,000 U) was administrated intramuscularly once a day for three consecutive days for anti-infection treatment. Two weeks later, operated SD rats were divided into 5 groups (n = 6):

Hulth model, Celecoxib, CS-semi5 50 mg/kg, CS-semi5 100 mg/kg, and CS-semi5 200 mg/kg groups. CS-semi5 was administered orally daily for 7 weeks. When the rats were sacrificed, the operated joints were assessed by magnetic resonance imaging (MRI) and micro-computed tomography (micro-CT) analysis.

### 2.16. Papain-induced OA in rats

The anti-OA activity of CS-semi5 was further investigated in an OA rat model induced by papain. In brief, the papain solution was an admixture of 2% papain and 0.03 mol/L L-cysteine at the proportion of 1:1 in volume. Then 50 μL papain solution was injected into both knee joints of SD rats on the 1st, 4th, and 7th day, respectively. The same volume of sterile saline solution was injected into both knee joints of rats in the control group (n = 6). On the 8th day, injected rats were divided into 5 groups (n = 6): Papain model, Celecoxib, CS-semi5 50 mg/kg, CS-semi5 100 mg/kg, and CS-semi5 200 mg/kg groups. CS-semi5 was administered orally daily for 30 days. The exercise ability was measured, and the rats were sacrificed at the end of the experiment. Serum was taken for the exosome analysis. The width of the knee joints was measured, and the joints were then removed and fixed in 4% paraformaldehyde for MRI, micro-CT, hematoxylin and eosin staining, and immunohistochemical analysis.

### 2.17. Running platform test to measure the exercise ability of rats

Each rat was trained to adapt to the running test one week before the end of the papain-induced OA experiment. The rats were placed individually on the running conveyor belt until each rat could move forward autonomously on the running platform instead of stopping or touching the tail electric ring on the conveyor belt. After the adaptive training, the rats were placed individually on the stationary conveyor belt and initiated to run *via* an electric shock. The number of electric shock times each rat ran within 2 min was recorded. All the tests were repeated three times.

### 2.18. Exosome analysis

Control group, Papain model group, and CS-semi5 group (200 mg/kg) rat sera were collected for exosome preparation and analysis. Filter-aided proteome preparation, enzymatic hydrolysis, liquid chromatography−mass spectrometery (LC−MS), and preliminary data analyses were performed by Wayen Biotechnology (Shanghai, China).

### 2.19. Histology and immunohistochemical analysis

Rat knee joints were embedded in paraffin, cut into 4-μm sections, and mounted on glass microscope slides. Serial sagittal sections were stained with hematoxylin and eosin. For immunohistochemistry, the sections were dewaxed and dehydrated by incubation in 3% hydrogen peroxide. Afterwards, the sections were blocked in 3% bovine serum albumin at room temperature for 30 min. Primary antibody incubation was performed overnight at 4 °C. Subsequently, secondary antibody incubation at 25 °C for 50 min and diaminobenzidine staining were performed.

## 2.20. MRI and micro-CT

Left joints from sacrificed rats were immediately scanned using an MRI machine (PharmaScan 70/16 US, Bruker). Image slices were reconstructed using Paravision 6.0.1. Micro-CT (Siemens Inveon, Germany) scans of left joints were then taken at the Institute of Laboratory Animal Science, Chinese Academy of Medical Sciences, Beijing (China). Cross-sectional images in three dimension and quantitative outcomes were determined with Inveon Research Workplace III software (Germany).

## 2.21. miRNA extraction and quantitative real-time PCR (qPCR)

miRNA isolation and extraction were conducted according to the manufacturer's instructions (Invitrogen). Stem loop primer of miRNA was used. The qPCR internal reference primers recognized U6 snRNA. Reverse transcription (RT) was performed under the following conditions: RT at 16 °C for 30 min, 42 °C for 30 min, termination reaction at 85 °C for 5 min, and preservation at 4 °C. The end product of the RT reaction was preserved at −20 °C. QPCR was performed under the following conditions: 95 °C for 10 min, 95 °C for 15 s and 40 cycles, 50 °C for 50 s, and preservation at 4 °C.

## 2.22. The effect of miR-122-5p on MMP13 expression in primary chondrocytes

Lipofectamine 2000 and the diluted miR-122-5p mimic were mixed at a ratio of 1:1 and incubated with primary chondrocytes at room temperature for 15 min. Then, the medium was replaced with fresh opti-MEM, and the cells were cultured at 37 °C for 3 h. The medium was then replaced with complete culture medium. The transfected cells were incubated with CS-semi5 or miR-122-5p inhibitor for another 24 h.

## 2.23. Statistical analysis

All the results in this study are presented as the mean ± standard error of mean (SEM) of at least three independent experiments. The sample size of each experiment is indicated in the corresponding figure legend. Statistical analyses were performed with GraphPad Prism version 8.0 (GraphPad Inc., La Jolla, CA, USA) using one-way ANOVA. $P$ values $< 0.05$ were considered to indicate significance.

## 3. Results

### 3.1. Structure−activity relationship analysis of CS-semi compounds

A series of sulfated CS-semi compounds (Fig. 1C) with different molecular weights were semi-synthesized from CS-A (Fig. 1B for synthesis route). Croton oil-induced ear edema experiments were performed to determine the anti-inflammatory activity of the CS-semi compounds. As shown in Fig. 1C and D, CS-semi compounds with different sulfation displayed different anti-inflammatory effects. Compared with the model group, CS-semi5 and CS-semi6 could effectively inhibit ear edema in mice and these compounds had moderate sulfation (20%−26%;

Fig. 1D). Among the CS-semi compounds, CS-semi5 had the best anti-inflammatory activity and was therefore determined as the candidate for further experiments. CS-semi5 also displayed better activity than natural CS-A, natural CS-E, and D-glucosamine (D-Glu) (Fig. 1E) and showed good dose-dependent activity (Fig. 1F).

The analgesic effect of CS-semi5 was measured by acetic acid-induced writhing and hot plate tests. In the hot plate test, CS-semi5 greatly increased the pain threshold and extended the reactive time in a dose-dependent manner (Fig. 1G). CS-semi5 (200 mg/kg) effectively reduced writhing dose-dependently (Fig. 1H) in the acetic acid-induced writhing test.

### 3.2. Protective effect of CS-semi5 on primary chondrocytes in the complement-induced killing test

The protective effect of CS-semi5 against complement-induced primary chondrocyte death was investigated using the CCK8 method. The addition of complement (NHS) decreased the viability of primary chondrocytes. Treatment with CS-semi5 significantly inhibited the effect of NHS (Fig. 1I and J). The results of Alcian blue staining in the complement-induced primary chondrocytes confirmed the protective effect of CS-semi5 on chondrocytes (Fig. 1K and L) These results indicate that CS-semi5 not only protects chondrocytes against complement-induced death but also improve the matrix accumulation.

### 3.3. CS-semi5 decreased the expression and secretion levels of MMP13 and increased the expression of aggrecan and COL II in primary chondrocytes

Primary chondrocytes were treated with different concentrations of CS-semi5, and cell viability was determined by CCK8 (Fig. 2A). CS-semi5 had no cytotoxicity on primary chondrocytes.

MMP13 plays key functions in the remodeling of bone formation and is important in OA development. With IL-1$\beta$ (10 ng/mL) stimulation for 24 h, CS-semi5 can significantly inhibit the secretion of MMP13 in primary chondrocytes (Fig. 2B). CS-semi5 can also inhibit the expression of MMP13 in a dose-dependent manner (Fig. 2C and D) while increasing the expression of aggrecan (ACAN) in primary chondrocytes (Fig. 2C and E). The immuno-fluorescence results also demonstrated that CS-semi5 could inhibit the expression of MMP13 (Fig. 2F). As a matrix metalloproteinase, the main biological function of MMP13 is to degrade the matrix. Therefore, after confirming the inhibition of CS-semi5 on expression and secretion levels of MMP13, we tested its effect on the substrates of MMP13, including aggrecan and COL II. As shown in Fig. 2G and H, CS-semi5 significantly increased the content of aggrecan and COL II in IL-1$\beta$ (10 ng/mL)-stimulated primary chondrocytes.

### 3.4. CS-semi5 showed therapeutic effects on the cartilage, joint bone damage, and subchondral bone destruction in modified Hulth OA rats

The schematic of the modified Hulth OA rat model establishment is shown in Fig. 3A. CS-semi5 had no obvious effects on rat weight (Fig. 3B). The knees with arthritis demonstrated obvious joint swelling during the pathological process of OA, and knee
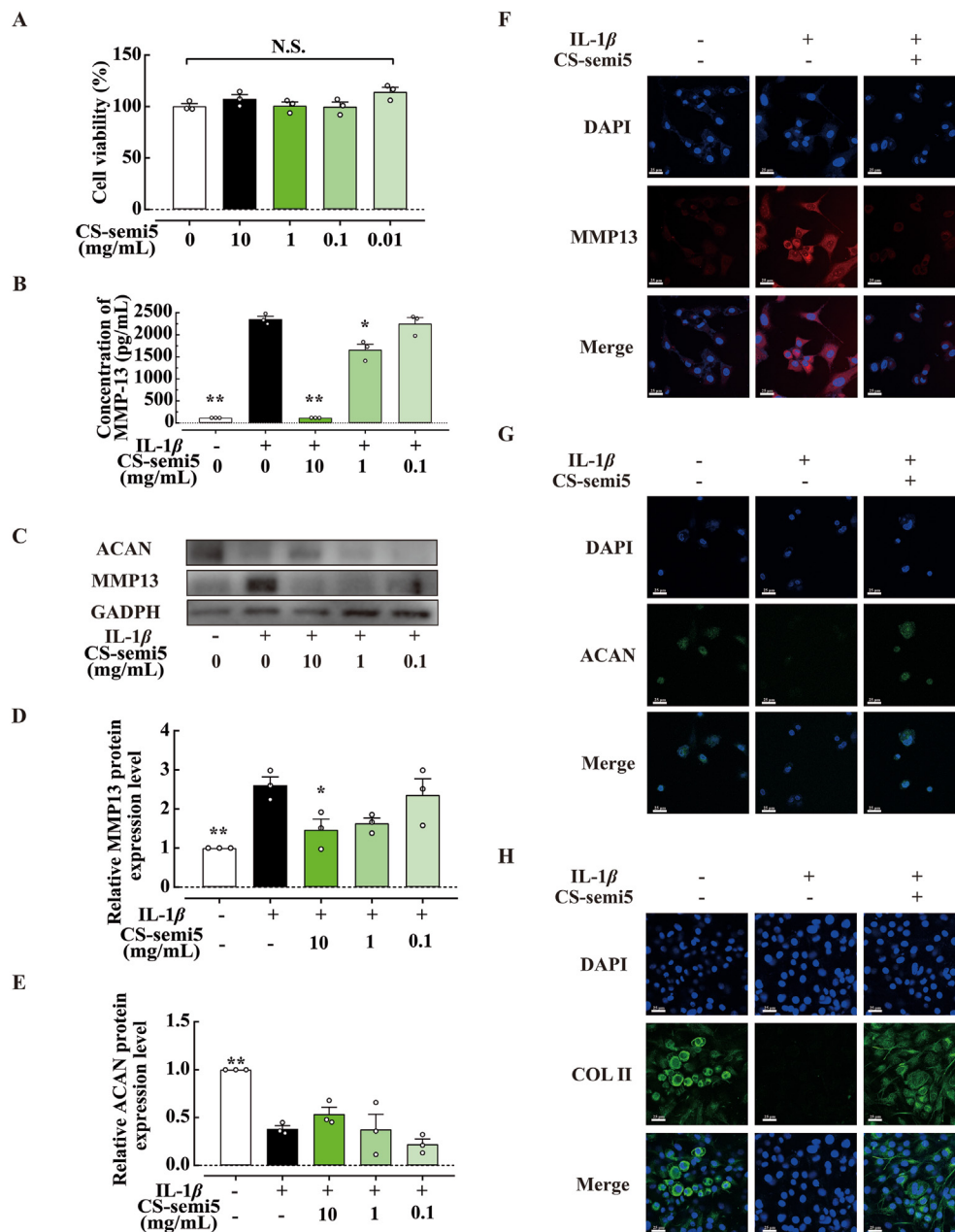
**Figure 2** CS-semi5 decreased MMP13 expression in primary chondrocytes. (A) CS-semi5 had no toxic effects on primary chondrocytes ($n = 3$). (B) ELISA demonstrated that CS-semi5 reduced MMP13 secretion in a dose-dependent manner ($n = 3$). Western blotting with quantitative results (C−E) and immunofluorescence analysis (F−H) indicated that CS-semi5 exerted cartilage-protective effects on MMP13, extracellular matrix components ACAN and COL II in IL-1$\beta$ (10 ng/mL)-stimulated primary chondrocytes ($n = 3$); *$P < 0.05$ and **$P < 0.01$ compared with the IL-1$\beta$ group; scale bar: 25 μm.

joint width measurements were taken to assess the anti-swelling effects of the compounds. CS-semi5 effectively inhibited swelling in the operated knee joint at the end of the experiment (Fig. 3C).

The cartilage surface of the joint cavity was observed to understand the damage to the knee joint cavity in rats. The surface of the femoral cartilage in the OA rats was dull and uneven, with narrow medial joint spaces and ulcers. In the positive control Celecoxib group, the articular cartilage surface was smooth, but the articular cavity structure was damaged. A dose-dependent improvement in knee joint structure was observed in the CS-

semi5-treated group, with complete and clear cartilage structure and smooth and flat cartilage surface (Fig. 3D).

MRI and Micro-CT are commonly used methods for clinically diagnosing and observing OA. MRI can be used to observe the integrity and functional status of articular cartilage. CS-semi5 can alleviate cartilage surface damage and subchondral bone sclerosis (Fig. 3E). The subchondral bone of the knee joint can be observed by micro-CT to assess remodeling. The patella of rats in the Celecoxib and CS-semi5 groups were close to the femoral platform, where a slight depression was formed at the joint in the CS-semi5 (50 and 100 mg/kg) group, while the high-
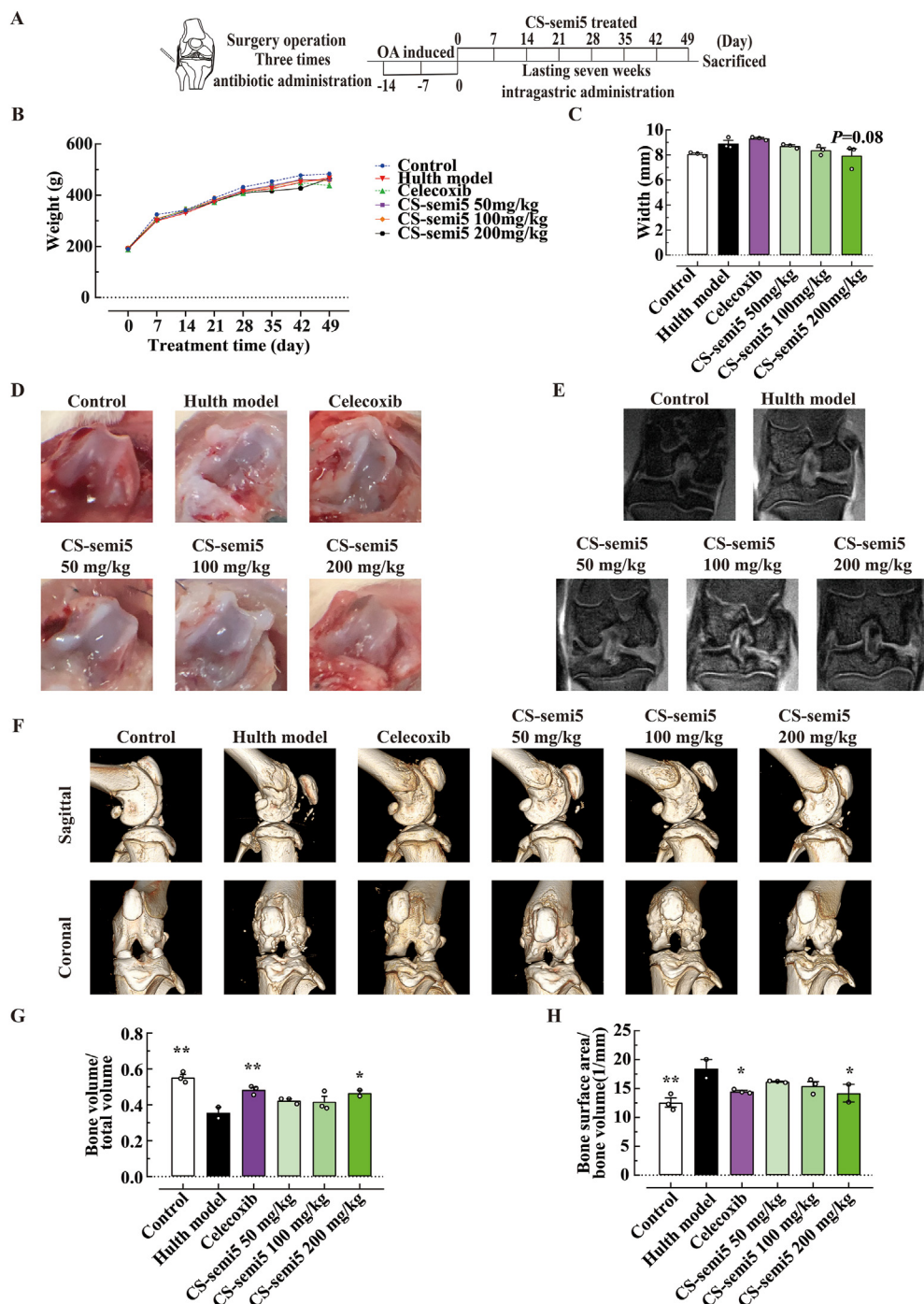
**Figure 3** CS-semi5 alleviated surgeon-induced OA in Hulth model rats ($n = 6$). (A) Schematic of the experimental process. (B) Weight changes of rats in all groups. (C) The width of the operated knee joint at the end of the experiment. (D) View of knee joint structure after operation and administration. (E) T1 MRI of operated joints. (F) Sagittal and coronal views of reconstructed joints. The quantitative outcomes of bone volume/total volume (G) and bone surface area/bone volume (H) measurements. **$P < 0.05$ and *$P < 0.01$ compared with the modified Hulth model group.

dose CS-semi5 group (200 mg/kg) demonstrated a significantly alleviated articular surface depression and improvement in bone joint deformation (Fig. 3F). These results indicate that CS-semi5 can improve joint damage and bone erosion in OA rats. The quantitative outcomes of bone volume/total volume and bone surface area/bone volume are shown in Fig. 3G and H, respectively.

### 3.5. CS-semi5 effectively alleviated joint swelling, improved mobility, and displayed a good cartilage protection effect in papain-induced OA rats

The schematic of papain-induced OA model development is shown in Fig. 4A. Compared with the model control group, there was no significant difference in the weight of animals in each

treatment group. Thus, CS-semi5 demonstrates no side effects regarding body weight in rats (Fig. 4B). The width of the left knee joint was measured, and CS-semi5 treatment significantly inhibited joint widening in comparison with that observed in the control model, indicating that CS-semi5 alleviates joint swelling (Fig. 4C).

In the previous OA experiments, the pain threshold of rats was measured using a mechanical stimulus; however, that approach does not reflect disrupted movement caused by pain in OA patients. Thus, a running platform was used to assess the rats' movement to determine the effects of OA knee joint pain on mobility. As the number of electric contacts increased, the rats' mobility decreased, indicating more severe OA. The average number of electric contacts of the OA model group was significantly higher than that of the control group, indicating that the mobility of OA rats was significantly reduced in comparison with that of normal rats. Compared with the model group, the number of electric contacts in the CS-semi5-treated groups (100
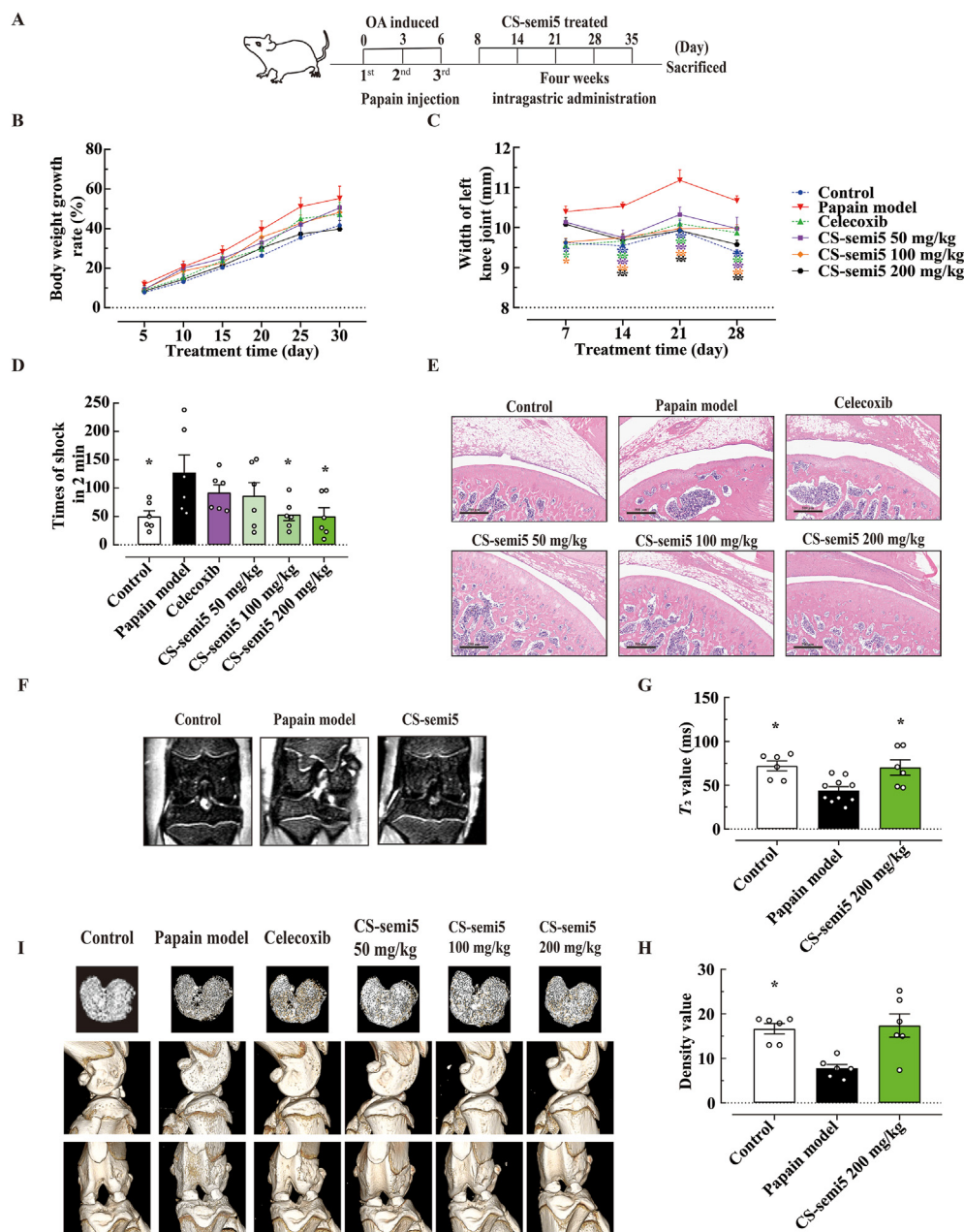


**Figure 4**  CS-semi5 alleviated papain-induced OA in rats ($n = 6$). (A) Schematic of the induction and treatment process. (B, C) show the weight changes and changes in the width of the left knee joint in rats during the experimental process. (D) Number of shocks in 2 min in the running test. (E) HE staining ($40 \times$); scale bar: 500 μm. (F) MRI of the junction between the femur and tibia in groups of control, papain-model, and CS-semi5 200 mg/kg. The T2 time (G) and density values (H) of MR images indicate joint water content. (I) The cross view of subchondral bone reconstruction on micro-CT with sagittal and coronal views of three-dimensional images of the knee joints. *$P < 0.05$ and **$P < 0.01$ compared with the Model group.

and 200 mg/kg) was significantly decreased, suggesting that CS-semi5 could relieve the knee joint pain symptoms of OA rats and significantly improve their mobility (Fig. 4D).

During the process of OA, the scattered matrix fragments trigger inflammation that damages the joint cartilage, making the cartilage surface uneven. As shown in Fig. 4E, knee joint HE staining revealed that the articular cartilage surface of control rats is smooth, and the chondrocytes are arranged smoothly. However, the articular cartilage surface of the model group was significantly less smooth than that of the control group. Compared with the papain-induced OA model group, the cartilage surface of the CS-semi5-treated group became smoother in a dose-dependent manner. This finding indicates that CS-semi5 can improve the damaged cartilage surface in OA rats.

The degree of joint cartilage injury was further assessed by MRI (Fig. 4F). Compared with that of the control group, the joint cartilage of the OA model group was more damaged, including a narrowed joint space, damaged or missing cartilage surface, an incomplete lateral cartilage edge, and reduced cartilage thickness. In the CS-semi5-treated group (200 mg/kg), the joint morphology was clear, and the joint space returned to normal. These findings indicate that CS-semi5 can effectively improve joint cavity injury in OA rats. Cartilage lesions are characteristic of the pathological process of OA, and the cartilage water content changes significantly when cartilage lesions occur. The measured gray and relaxation values on MRI were quantified to determine the change in cartilage water content. As shown in Fig. 4G and H, compared with those in the model group, the water content values in the articular cartilage of the CS-semi5-treated group were significantly higher, indicating that CS-semi5 can significantly increase the water content of articular cartilage.

Micro-CT images of the subchondral bone and whole joints of rats in each group are shown in Fig. 4I. Compared with that in the rats in the control group, the subchondral bone of the knee joint in OA model rats displayed bone destruction, serious erosion, obvious cavity formation in the joint, and deformation of the bone joint. Celecoxib and CS-semi5 (50 mg/kg) slightly improved this bone destruction and erosion, whereas CS-semi5 (100 and 200 mg/kg) had a significant effect and reduced the regional wear range of the tibia. These findings indicate that CS-semi5 can alleviate joint bone damage to some extent. To further explore the role of CS-semi5 in reducing bone destruction, we analyzed the relevant indicators of bone mineral density, including bone volume/total volume, bone surface area/bone volume, trabecular thickness, trabecular spacing, trabecular number, trabecular pattern factor, and cortical wall thickness. CS-semi5 delayed trabecular bone loss in model rats to a certain extent but had little effect on bone mineral density and cortical bone (Supporting Information Fig. S1).

### 3.6. Preliminary safety evaluation of CS-semi5

Preliminary tests were conducted to assess CS-semi5 safety. The acute toxicity test of CS-semi5 was conducted in ICR mice by oral administration of up to 5 g/kg. Subacute oral toxicity analysis was performed in SD rats for four consecutive weeks by oral administration of CS-semi5 (100 and 500 mg/kg). During the experimental period, body weight, behavior, and adverse signs of toxicity were observed. At the end of the experiment, all rats were anesthetized for the collection of blood samples for hematological and biochemical analysis. The organs, including the heart, liver, spleen, lung, and kidney, were removed for histopathological analysis. CS-semi5 had no obvious effect on the weight and organ

coefficients of the rats after four consecutive weeks of treatment (Fig. 5A and B). The HE results also confirmed that CS-semi5 had no toxic effects on major organs, including the heart, liver, spleen, lung, and kidney (Fig. 5C). CS-semi5 also had no adverse effects on hematological indicators, biochemical factors, or coagulation function.

### 3.7. Screening and confirmation of miR-122-5p as a key regulator in CS-semi5 treatment

The serum exosome analysis of OA rats revealed numerous microRNAs (Fig. 6A). microRNAs were compared and visualized in a Venn diagram, revealing seven differentially expressed microRNA genes (Fig. 6B). Among them, six were upregulated and one was downregulated by CS-semi5. The upregulated microRNAs were miR-122-5p, miR-466c-5p, miR-881-3p, miR-326-5p, miR-328a-5p, and miR-3473. Downregulated miRNA was let-7d-5p. Reviewing the literature, the expression ratio in these groups, GEO database prediction results (Supporting Information Fig. S2A), and homology verification, we determined that CS-semi5 may exert anti-OA activity by upregulating miR-122-5p. We further confirmed our assumption in primary chondrocytes. IL-1$\beta$ greatly inhibited the expression of miR-122-5p in primary chondrocytes, and CS-semi5 reversed the miR-122-5p downregulation induced by IL-1$\beta$ (Fig. 6C).

The intersection predictions between MiRanda and miRPathDB software included 2323 target genes regulated by miR-122-5p in the OA model (Fig. S2B). Then we screened the related target genes that can regulate MMP13 based on our previous experimental results. The molecular network map of target genes regulated by miR-122-5p and interacting with MMP13 was obtained (Fig. 6D left). By analyzing the molecular network map on the principle of base complementary, we revealed that the protein most closely related to MMP13 is MAPK14, i.e., p38, which can also interact with miR-122-5p. The 3′UTR of p38 mRNA has a total length of 2079 bp (NCBI Reference Sequence: NM_001168508.1). We predicted the binding site of miR-122-5p and p38, and the specific analysis results are shown in Fig. 6D (right).

Then we verified the binding specificity of miR-122-5p to the p38 3′UTR region with a double luciferase reporter gene experiment. The p38 3′UTR target gene was constructed into the 3′ end of the luciferase gene. As shown in Fig. 6E, the expression of firefly luciferase in cells transfected with p38 Mapk14 3′UTR reporter plasmid was detected, and that of cells transfected with the miR-122-5p mimic was significantly lower than that those transfected with the mimic control. These results suggest that miR-122-5p can specifically bind to the p38 3′UTR region.

### 3.8. CS-semi5 inhibited the expression of MMP13 and its substrate protein via miR-122-5p/p38

Firstly, the effect of miRNA was verified by using miRNA mimics and miRNA inhibitors (Supporting Information Fig. S3). Then relative MMP13 expression level was detected by qPCR in IL-1$\beta$ induced chondrocytes treated with CS-semi5 treatment with or without the miR-122-5p inhibitor (Fig. 6F). CS-semi5 could inhibit MMP13 and miR-122-5p inhibitor could inverse the inhibitory effect, which denoted that CS-semi5 maybe inhibit MMP13 by miR-122-5p.

The inhibitory effect of CS-semi5 on p38 expression was also measured (Fig. 6G and H). CS-semi5 also decreased expression of p-p38 in IL-1$\beta$ induced chondrocytes with CS-
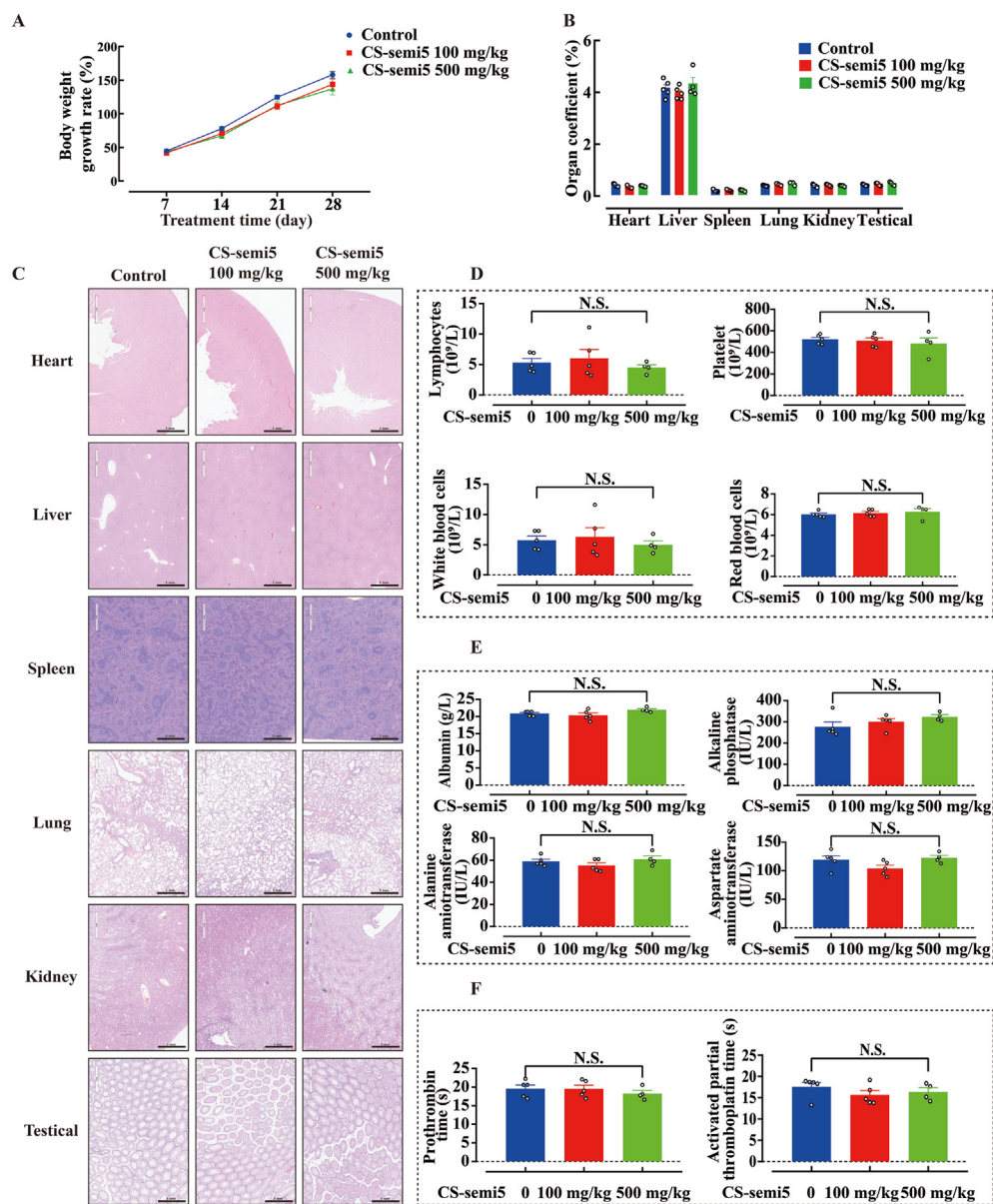
**Figure 5** Preliminary safety evaluation of CS-semi5 (100 and 500 mg/kg) ($n = 5$). (A) The effect of CS-semi5 on the body weight of rats. (B) The effect of CS-semi5 on the main organ coefficient of rats. (C) HE staining of main organs, including the heart, liver, spleen, lung, kidney, and testicles; scale bar: 1 mm. (D) Hematological, (E) biochemical, and (F) coagulation function analyses of rat blood after 4 weeks of treatment with CS-semi5 at 100 and 500 mg/kg. N.S., no significance between control and treatment groups.

semi5 treatment. To determine whether CS-semi5 could inhibit MMP13 by p38 pathway, SB203580, a specific inhibitor of p38, was added into IL-1$\beta$ induced chondrocytes with CS-semi5 treatment. The inhibition effect of CS-semi5 on MMP13 was synergized by SB203580, suggesting that CS-semi5 had a combined inhibitory effect on the downstream MMP13 *via* p38 (Fig. 6I).

The main content of the cartilage matrix is COL II and aggrecan, which is also the substrate of MMP13. As shown in Fig. 6J, the addition of CS-semi5 alone can increase the expression of COL II; however, after adding the miR-122-5p inhibitor, this effect disappeared. This finding confirms that CS-semi5 specifically increases the expression of downstream COL II through miR-122-5p. Overall, the above results indicate that CS-semi5 upregulates miR-122-5p, inhibiting the expression of

p38 and MMP13 and then increasing the level of downstream substrates.

Finally, p38, MMP13, and substrate protein levels were detected by IHC (Fig. 7) in the articular cartilage of papain-induced OA rats, confirming that CS-semi5 effectively inhibited the expression of p38 and MMP13 and increased COL II levels in OA rats.

## 4. Discussion

Due to the heterogeneity and structural complexity of polysaccharide molecules, the study of polysaccharide compounds and their mechanisms, as well as drug applications, has always been a hot and difficult research topic. Polysaccharide CS has been prescribed as symptomatic slow-acting drugs for treating OA
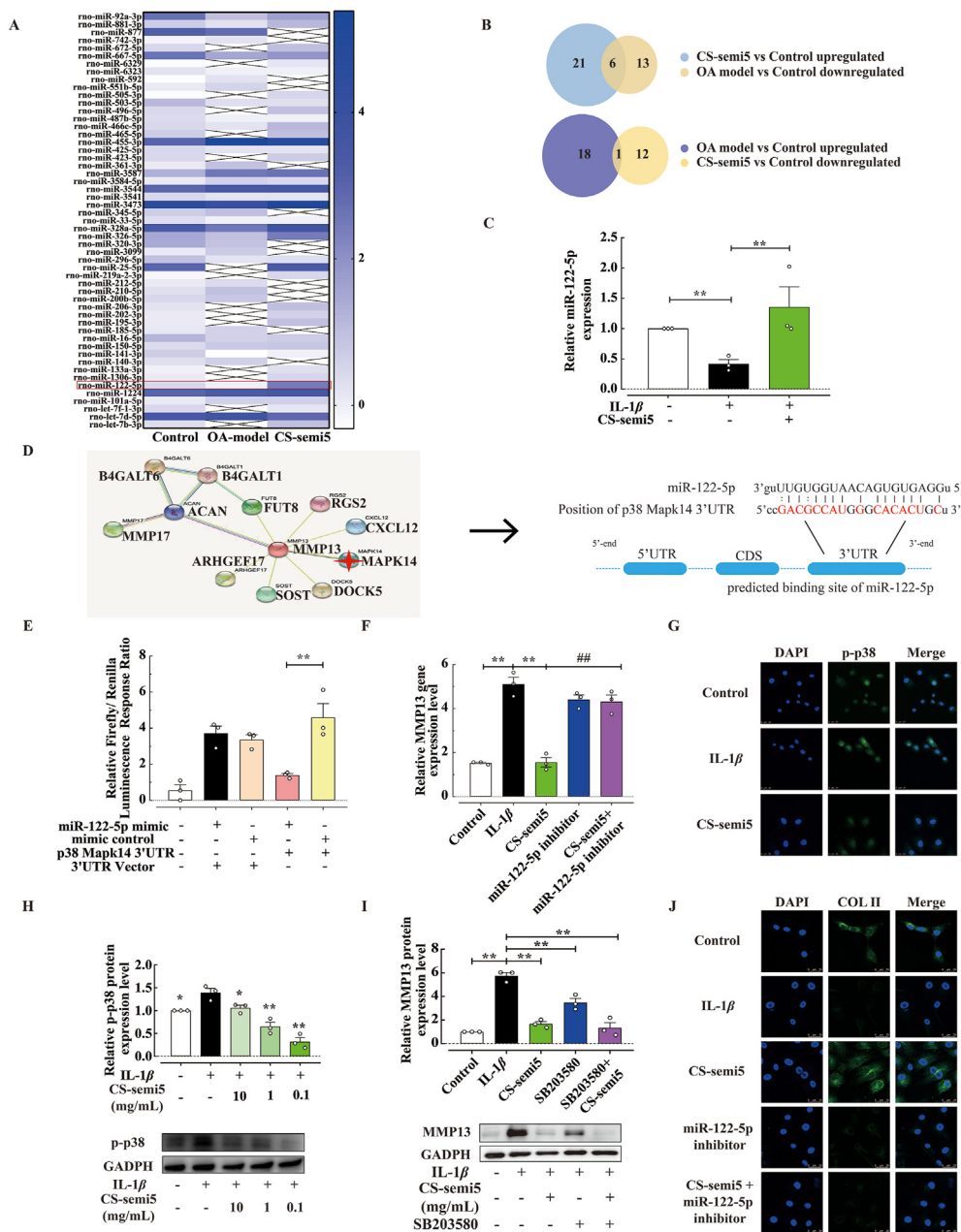
**Figure 6** The molecular mechanism by which CS-semi5 treats OA ($n = 3$). (A) Heatmap showing the different microRNA levels in the control, papain model, and CS-semi5 treatment groups. (B) Venn diagram showing differentially expressed genes in the different groups. (C) CS-semi5 increased miR-122-5p expression in IL-1$\beta$ induced chondrocytes, as demonstrated by qPCR. **$P < 0.01$ compared with the IL-1$\beta$-induced model group. (D) The interaction network of target genes for MMP13 and predicted potential binding site of *Mapk14* 3′UTR mRNA. (E) Luciferase activity in 293T cells transfected with a dual luciferase reporter gene with the miR-122-5p mimic. **$P < 0.01$ compared with the group added miR-122-5p mimic. (F) Relative *Mmp13* expression level by qPCR in IL-1$\beta$ induced chondrocytes treated with CS-semi5 treatment with or without the miR-122-5p inhibitor. Immunofluorescence (G) and protein blotting (H) of p-p38 in IL-1$\beta$ induced chondrocytes with CS-semi5 treatment; scale bar: 25 μm. Western blotting (I) of MMP13 (upper) and quantification (lower) in IL-1$\beta$ induced chondrocytes treated with CS-semi5 with or without p38 inhibitor SB230580. **$P < 0.01$ compared with the IL-1$\beta$-induced model group, ##$P < 0.01$ compared with the CS-semi5 treated model group. (J) Immunofluorescence of COL II expression in IL-1$\beta$ induced chondrocytes treated with CS-semi5 with or without the miR-122-5p inhibitor; scale bar: 25 μm.

in European countries since 1984, whereas they are sold only as nutraceuticals in the USA[5]. Whether CS products are drugs or nutraceuticals remains uncertain due to the inconsistent therapeutic effects observed across different clinical trials[8,9]. These different effects arise from CS differences regarding the position and degree of sulfation of the CS sugar chain, which alters

biological functions. The fine structure of CS determines the function of polysaccharides and the specificity of interactions with various protein molecules[10]. CS (Fig. 1A) can be divided into multiple subtypes and demonstrates sulfation pattern variation, resulting in the high heterogeneity and complexity of CS from different sources. Commercial CS is generally derived from
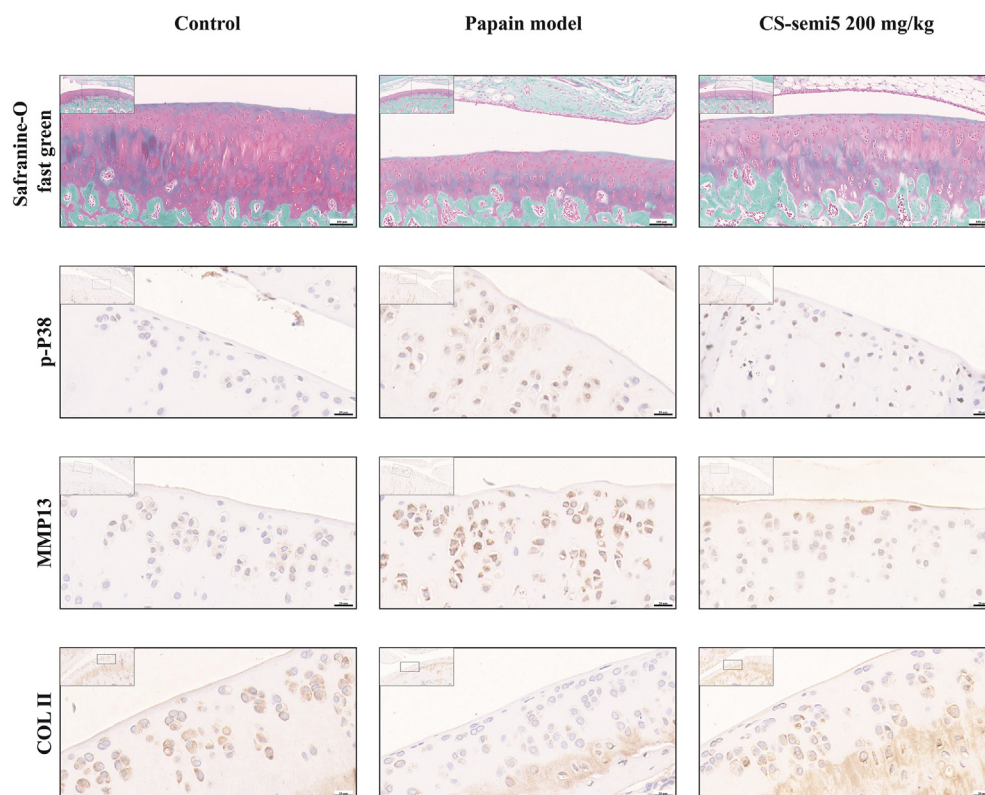
**Figure 7**  CS-semi5 inhibits the p38−MMP13 axis in the articular cartilage of OA rats. Immunohistochemical images of papain-induced OA rats show that CS-semi5 reduced p-p38 and MMP13 levels and increased COL II levels in the cartilage *vs.* those observed in the model groups, scale bar: 100 μm in safranine-O fast green staining images, 20 μm in immunohistochemical images.

bovine or porcine cartilage, which is rich in CS-A; however, CS-A has low bioactivity. CS-E can promote osteoblast differentiation, inhibit osteoclasts, increase bone mineralization, and exert other bone-protective biological activities. However, CS-E can only be obtained from squid cartilage, and the extraction and purification process are challenging[11].

The structure of CS-E is [4)-$\beta$-D-GlcA-(1−3)-$\beta$-D-4,6-$O$-disulfate-GalNAc-(1−]$_n$. We previously synthesized CS-E tetra-, hexasaccharides, and glycodendrimers and evaluated their biological activities. Based on our previous findings, we speculated that the degree and position of sulfation are related to CS biological activity. In this paper, CS polysaccharides with different degrees of sulfation were prepared according to previously described methods for CS oligosaccharide synthesis. We conducted a structure−activity relationship study and identified the most active polysaccharide compound CS-semi5. The croton oil-induced ear swelling model was used to evaluate the anti-inflammatory activity of this series of CS-Es synthesized from CS-A *in vivo* in mice. In the structure−activity relationship study, CS-semi5 exhibited better anti-inflammatory effects in a dose-dependent manner than the other CS polysaccharides and D-Glu (Fig. 1D−F). Additionally, CS-semi5 demonstrated a good analgesic effect, which is beneficial since OA can cause pain (Fig. 1G and H). Critically, CS-semi5 protected primary chondrocytes against complement-induced death (Fig. 1I−L). Overall, these findings preliminarily confirmed that CS-semi5 acts as an anti-inflammatory, analgesic, and cartilage-protective agent superior to the other available drugs for treating OA.

OA is a chronic disease characterized by cartilage degeneration. Although the pathogenesis of OA has not been fully elucidated, the mechanism of cartilage degradation has been extensively investigated, and it is now believed that extracellular matrix synthesis and degradation in articular chondrocytes is greatly imbalanced in OA[12,13]. The main characteristic of OA pathology is the progressive degradation of the extracellular matrix. MMP-13 is one of the main contributors to cartilage extracellular matrix decomposition during OA pathogenesis in OA patients and animal models. MMP-13 participates in cartilage damage mainly by enzymatically degrading cartilage proteoglycan and collagen[14,15]. To further validate the possible protective effect of CS-semi5 on chondrocytes, we investigated its role in the extracellular cartilage matrix *in vitro* (Fig. 2). CS-semi5 inhibited the expression and secretion of MMP13, thereby increasing the aggrecan and COL II content. Thus, CS-semi5 can effectively promote cartilage matrix synthesis and relieve the pathological state of cartilage matrix decomposition and synthesis imbalance.

The clinical manifestations of OA are joint pain, tenderness, stiffness, joint swelling, limited mobility, and joint deformity[2]. The anti-OA effect of CS-semi5 was evaluated respectively in modified Hulth OA rats and papain-induced OA rats. CS-semi5 showed significant anti-swelling activity and greatly improved arthritic pain sensitivity in OA rats, thereby improving their mobility. Regarding cartilage protection, CS-semi5 improved the knee joint structure and promoted cartilage damage repair in a dose-dependent manner. Overall, our findings indicate that CS-semi5 has both cartilage protection and anti-inflammatory activities. Notably, CS-semi5 had greater analgesic effects than the positive control drug celecoxib and cartilage protection agent glucosamine, further indicating the advantage of CS-semi5 for OA treatment (Figs. 3 and 4).

Preliminary tests were conducted to assess CS-semi5 safety (Fig. 5). The acute toxicity of CS-semi5 was >5 g/kg by oral administration; the subacute oral toxicity analysis revealed no toxicity to rats administered CS-semi5 orally for four consecutive weeks. CS-semi5 demonstrated no adverse effects on weight or obvious toxicity to major organs after one month of administration *in vivo*. No abnormal hematological or biochemical findings were observed. Thus, CS-semi5 demonstrated good safety.

We further investigated the mechanism by which CS-semi5 exerted its anti-OA effect (Fig. 6). MicroRNA has been reported to play an important role in the pathogenesis of OA[16]. On the one hand, adipocytes, osteoblasts, and chondrocytes are the three main lineages that differentiate mesenchymal stromal cells (MSCs), and these differentiation pathways are strictly regulated by microRNAs[17]. MicroRNAs such as miR-125a-5p, miR-320e, and miR-135-5p can promote bone formation[18−20]. Studies have shown that two microRNAs specifically enhance chondrogenesis: miR-455-3p and miR-193b-3p[21,22]. On the other hand, microRNA affects the occurrence and development of OA by regulating cartilage homeostasis. In human OA cartilage, the expression of miR-17 is significantly lower than that in normal tissues. The downregulation or overexpression of miR-17 in mice can accelerate or delay, respectively, the occurrence and development of OA diseases[23]. Some studies have demonstrated that miR-27a and miR-27b have similar regulatory effects, and their expression in OA chondrocytes decreases, accompanied by an increased expression of IGFBP5 and MMP13[24,25]. Treatment strategies involving microRNAs have also emerged, such as transplanting cartilage particles from human bone marrow cells, which overexpress beneficial microRNAs (such as miR-92a-3p) enhancing chondrogenesis[26,27].

Here, we used bioinformatics tools to analyze microRNAs related to OA and investigate possible anti-OA mechanisms and targets of CS-semi5 (Figs. 6 and 7). We first used the GEO database to screen the microRNA expression pattern in OA cartilage tissue (Fig. S2). Then, the results of exosomomics revealed seven differentially expressed microRNAs. Combining the aforementioned results revealed that CS-semi5 might play an anti-OA role by upregulating miR-122-5p (Fig. 6A and B).

miR-122-5p has been proved to play an important role in many diseases including cardiovascular disease, neuroinflammation, skin disease and so on. Wang et al.[28] found that the expression of IL-1β and TNF-α were negatively correlated with the level of miR-122-5p in activated BV2 cells and astrocytes. Wang et al.[29] reported that miR-122-5p could be as a target for regulating melanogenesis. Besides, it has been reported that exosome-carried miRNAs (miR-125b-5p, miR-122-5p, miR-342-5p, miR-126, miR-130a, miR-138-5p, and miR-455) mainly regulate the expression of MAPK, NF-κB, VEGF, and Caspase and then protect the cardiovascular system[30]. Li et al.[31] found that hUCMSCs-EVs can alleviate cartilage degradation by enriching miRNAs, including has-miR-122-5p, has-miR-148a-3p, has-miR-486-5p, and has-miR-let-7a-5p, during OA progression. Alahdal et al.[32] reported that IDO1 overexpression in the synovial fluid of OA patients impaired the chondrogenic differentiation of MSCs and cartilage regeneration through the downregulation of miR-122-5p. These related studies indicated that miR-122-5p also plays an important role in cartilage damage and regeneration. Thus, we explored and proved that CS-semi5 could upregulate the expression of miR-122-5p in IL-1β-stimulated primary chondrocytes (Fig. 6C).

Next, the regulatory target gene of miR-122-5p was predicted by STRING molecular interaction, revealing p38 MAPK14 as the effector molecule of CS-semi5 by establishing the regulatory network of target genes. A luciferase double reporter gene experiment confirmed that miR-122-5p could directly bind to the 3′UTR region of p38 MAPK14, revealing that CS-semi5 regulated p38 MAPK14 through miR-122-5p to produce anti-OA effects (Fig. 6D).

Among the miR-122-5p binding target genes, p38 MAPK14 interacts closely with MMP13, suggesting that miR-122-5p may inhibit MMP13 by regulating p38 MAPK14, thereby affecting cartilage degradation[33]. Thereby, we confirmed CS-semi5 could inhibit the expression of p38 and then MMP13 (Fig. 6F−H). We then confirmed that CS-semi5 could indeed inhibit the expression of MMP13 by upregulating miR-122-5p using miR-122-5p and p38 inhibitors (Fig. 6I and J), subsequently increasing substrate protein COL II (Fig. 6K) *in vitro*. CS-semi5 was also shown to inhibit the expression of p38, MMP13 and increase COL II levels with good cartilage protective effect *in vivo* (Fig. 7).

The CS-semi5 prepared from CS-A in this study not only improves the cartilage protection activity of natural CSE but also has anti-inflammatory and analgesic characteristics. These properties fill the gap in OA drug treatment, with the common activity of non-steroidal anti-inflammatory drugs (such as celecoxib) and cartilage protective drugs (such as glucosamine). Because of the complexity of the polysaccharide chain, the activity and mechanism of CS-semi5 is very complex, we will further explore other transcription factors related to miR-122-5p and downstream cartilage protection regulation mechanisms in other paper. In addition to miR-122-5p, the complement pathway, chemokine receptor and other molecules all contribute to the effect of CS-semi5 on OA (unpublished data). In the future, we will also investigate other relevant anti-OA mechanisms of CS-semi5.

## 5. Conclusions

This study offers a new semi-synthesis method for preparing large amounts of CS-E (*i.e.*, CS-semi5) with good anti-OA bioactivity, solving the problem of limited natural CSE resources and unstable quality sources in clinical practice. This study also investigates for the first time the mechanism by which CS-semi5 can upregulate miR-122-5p, inhibit the p38/MMP13 pathway, and ultimately alleviate cartilage degeneration during OA pathogenesis. The semi-synthetic CS-semi5 not only demonstrated good safety but also greatly improved anti-inflammatory and analgesic characteristics and protected cartilage in comparison with the effects of natural chondroitin sulfate, celecoxib and cartilage protection agent glucosamine, which fills the gap in OA drug treatment strategies and meets an urgent clinical need, thus making CS-semi5 a promising anti-OA candidate superior to most available drugs.

## Author contributions

Xiang Li: Writing − original draft, Investigation. Ya Zhou: Writing − original draft, Validation, Investigation. Xuefeng Chen: Visualization, Formal analysis, Data curation. Hongjun Wang:

Methodology, Formal analysis, Data curation. Shuang Yang: Methodology. Jun Yang: Resources, Methodology. Yunfeng Song: Investigation. Zhehui Zhao: Visualization, Project administration, Conceptualization. Haijing Zhang: Writing − review & editing, Project administration, Data curation, Conceptualization. Lianqiu Wu: Writing − review & editing, Supervision, Funding acquisition, Conceptualization.

## Conflicts of interest

The authors declare no competing interests.

## Appendix A.   Supporting information

Supporting information to this article can be found online at https://doi.org/10.1016/j.apsb.2024.05.016.

## References

1. Allen KD, Thoma LM, Golightly YM. Epidemiology of osteoarthritis. *Osteoarthritis Cartilage* 2022;**30**:184−95.
2. Li D, Li S, Chen Q, Xie X. The prevalence of symptomatic knee osteoarthritis in relation to age, sex, area, region, and body mass index in China: a systematic review and meta-analysis. *Front Med* 2020;**7**: 304.
3. Bishnoi M, Jain A, Hurkat P, Jain SK. Chondroitin sulphate: a focus on osteoarthritis. *Glycoconj J* 2016;**33**:693−705.
4. Martel-Pelletier J, Farran A, Montell E, Vergés J, Pelletier JP. Discrepancies in composition and biological effects of different formulations of chondroitin sulfate. *Molecules* 2015;**20**:4277−89.
5. Wang K, Qi L, Zhao L, Liu J, Guo Y, Zhang C. Degradation of chondroitin sulfate: mechanism of degradation, influence factors, structure−bioactivity relationship and application. *Carbohydr Polym* 2023;**301**:120361.
6. Pomin VH. Sulfated glycans in inflammation. *Eur J Med Chem* 2015; **92**:353−69.
7. Sharma R, Kuche K, Thakor P, Bhavana V, Srivastava S, Mehra NK, et al. Chondroitin sulfate: emerging biomaterial for biopharmaceutical purpose and tissue engineering. *Carbohydr Polym* 2022;**286**:119305.
8. Kolasinski SL, Neogi T, Hochberg MC, Oatis C, Guyatt G, Block J, et al. 2019 American College of Rheumatology/Arthritis Foundation guideline for the management of osteoarthritis of the hand, hip, and knee. *Arthritis Rheumatol* 2020;**72**:220−33.
9. Arden NK, Perry TA, Bannuru RR, Bruyère O, Cooper C, Haugen IK, et al. Non-surgical management of knee osteoarthritis: comparison of ESCEO and OARSI 2019 guidelines. *Nat Rev Rheumatol* 2021;**17**: 59−66.
10. Höök M, Kjellén L, Johansson S, Robinson J. Cell-surface glycosaminoglycans. *Annu Rev Biochem* 1984;**53**:847−69.
11. Restaino OF, Schiraldi C. Chondroitin sulfate: are the purity and the structural features well assessed? A review on the analytical challenges. *Carbohydr Polym* 2022;**292**:119690.
12. Hunter DJ, Bierma-Zeinstra S. Osteoarthritis. *Lancet* 2019;**393**: 1745−59.
13. He L, Xu Z, Niu X, Li R, Wang F, You Y, et al. GPRC5B protects osteoarthritis by regulation of autophagy signaling. *Acta Pharm Sin B* 2023;**13**:2976−89.
14. Wang M, Sampson ER, Jin H, Li J, Ke QH, Im HJ, et al. MMP13 is a critical target gene during the progression of osteoarthritis. *Arthritis Res Ther* 2013;**15**:R5.
15. Li H, Wang D, Yuan Y, Min J. New insights on the MMP-13 regulatory network in the pathogenesis of early osteoarthritis. *Arthritis Res Ther* 2017;**19**:248.
16. Tong L, Yu H, Huang X, Shen J, Xiao G, Chen L, et al. Current understanding of osteoarthritis pathogenesis and relevant new approaches. *Bone Res* 2022;**10**:60.
17. Chen Q, Shou P, Zheng C, Jiang M, Cao G, Yang Q, et al. Fate decision of mesenchymal stem cells: adipocytes or osteoblasts?. *Cell Death Differ* 2016;**23**:1128−39.
18. Sun L, Lian JX, Meng S. MiR-125a-5p promotes osteoclastogenesis by targeting TNFRSF1B. *Cell Mol Biol Lett* 2019;**24**:23.
19. Yin N, Zhu L, Ding L, Yuan J, Du L, Pan M, et al. MiR-135-5p promotes osteoblast differentiation by targeting HIF1AN in MC3T3-E1 cells. *Cell Mol Biol Lett* 2019;**24**:51.
20. Xu C, Zhang Z, Liu N, Li L, Zhong H, Wang R, et al. Small extracellular vesicle-mediated miR-320e transmission promotes osteogenesis in OPLL by targeting TAK1. *Nat Commun* 2022;**13**: 2467.
21. Meng F, Li Z, Zhang Z, Yang Z, Kang Y, Zhao X, et al. MicroRNA-193b-3p regulates chondrogenesis and chondrocyte metabolism by targeting HDAC3. *Theranostics* 2018;**8**:2862−83.
22. Chen W, Chen L, Zhang Z, Meng F, Huang G, Sheng P, et al. MicroRNA-455-3p modulates cartilage development and degeneration through modification of histone H3 acetylation. *Biochim Biophys Acta* 2016;**1863**:2881−91.
23. Zhang Y, Li S, Jin P, Shang T, Sun R, Lu L, et al. Dual functions of microRNA-17 in maintaining cartilage homeostasis and protection against osteoarthritis. *Nat Commun* 2022;**13**:2447.
24. Akhtar N, Rasheed Z, Ramamurthy S, Anbazhagan AN, Voss FR, Haqqi TM. MicroRNA-27b regulates the expression of matrix metalloproteinase 13 in human osteoarthritis chondrocytes. *Arthritis Rheum* 2010;**62**:1361−71.
25. Tardif G, Hum D, Pelletier J-P, Duval N, Martel-Pelletier J. Regulation of the IGFBP-5 and MMP-13 genes by the microRNAs miR-140 and miR-27a in human osteoarthritic chondrocytes. *BMC Muscoskel Disord* 2009;**10**:148.
26. Mao G, Zhang Z, Hu S, Zhang Z, Chang Z, Huang Z, et al. Exosomes derived from miR-92a-3p-overexpressing human mesenchymal stem cells enhance chondrogenesis and suppress cartilage degradation *via* targeting WNT5A. *Stem Cell Res Ther* 2018;**9**:247.
27. Zhao T, Li X, Li H, Deng H, Li J, Yang Z, et al. Advancing drug delivery to articular cartilage: from single to multiple strategies. *Acta Pharm Sin B* 2022;**13**:4127−48.
28. Wang H, Li Y, Jiang S, Liu N, Zhou Q, Li Q, et al. LncRNA xist regulates sepsis associated neuroinflammation in the periventricular white matter of CLP rats by miR-122-5p/PKCη axis. *Front Immunol* 2023;**14**:1225482.
29. Wang J, Li Y, Feng C, Wang H, Li J, Liu N, et al. Peptide OA-VI12 restrains melanogenesis in B16 cells and C57B/6 mouse ear skin *via* the miR-122-5p/Mitf/Tyr axis. *Amino Acids* 2023;**55**: 1687−99.
30. Lai Z, Liang J, Zhang J, Mao Y, Zheng X, Shen X, et al. Exosomes as a delivery tool of exercise-induced beneficial factors for the prevention and treatment of cardiovascular disease: a systematic review and meta-analysis. *Front Physiol* 2023;**14**:1190095.
31. Li K, Yan G, Huang H, Zheng M, Ma K, Cui X, et al. Anti-inflammatory and immunomodulatory effects of the extracellular vesicles derived from human umbilical cord mesenchymal stem cells on osteoarthritis *via* M2 macrophages. *J Nanobiotechnol* 2022;**20**:38.
32. Alahdal M, Huang R, Duan L, Zhiqin D, Hongwei O, Li W, et al. Indoleamine 2,3 dioxygenase 1 impairs chondrogenic differentiation of mesenchymal stem cells in the joint of osteoarthritis mice model. *Front Immunol* 2021;**12**:781185.
33. Sondergaard BC, Schultz N, Madsen SH, Bay-Jensen AC, Kassem M, Karsdal MA. MAPKs are essential upstream signaling pathways in proteolytic cartilage degradation—divergence in pathways leading to aggrecanase and MMP-mediated articular cartilage degradation. *Osteoarthritis Cartilage* 2010;**18**:279−88.